

SUPPORTING INFORMATION

Superior CO₂ Uptake on N-doped Activated Carbon through Hydrogen-Bonding Interaction

Wei Xing, * Chao Liu, Ziyan Zhou, Lei Zhang, Jin Zhou, Shuping Zhuo, * Zifeng Yan, * Hong Gao, Guiqiang Wang, Shi Zhang Qiao *

[*] Prof. W. Xing, Mr. C. Liu, Prof. Z. Zhou, Dr. J. Zhou, Prof. S. Zhuo, Prof. G. Wang

School of Chemical Engineering, Shandong University of Technology
Zibo 255049 (P. R. China)

E-mails: xingwei@sdut.edu.cn, zhuosp@sdut.edu.cn

Dr. L. Zhang, Dr. H. Gao
State Key Laboratory of Catalysis
Dalian Institute of Chemical Physics, Chinese Academy of Science, 457 Zhongshan Road, Dalian 116023 (P. R. China)

Prof. Z. F. Yan
State Key Laboratory of Heavy Oil Processing
Key Laboratory of Catalysis, CNPC
School of Chemical Engineering, China University of Petroleum, 66, Changjiang West Road
Qingdao 266580 (P. R. China)
Email: zfyancat@upc.edu.cn

Prof. S. Z. Qiao
School of Chemical Engineering
The University of Adelaide, SA5005 (Australia)
Email: s.qiao@adelaide.edu.au

Content

Table S1 Surface areas and pore-structure parameters of the activated carbons

Table S2 Surface composition of the activated carbons

Table S3 The total energies for NCSM-CO₂ and CSM-CO₂ complexes

Figure S1 N₂ adsorption isotherms for all the carbons investigated

Figure S2 SEM images of (a) SK-0.5-700 and (b) SK-4-700

Figure S3 The plot of CO₂ adsorption capacity per unit surface area and imaginary CO₂ monolayer coverage on the surface of carbon versus the nitrogen content of the carbons

Figure S4 A plot of CO₂ adsorption capacities vs. oxygen contents of the carbons

Figure S5 Geometric configurations and total energies for NCSM, CSM, NCSM-CO₂ complexes and CSM-CO₂ complexes

Figure S6 FT-IR spectra of the activated carbon measured under different atmosphere

Figure S7 Isosteric heats of CO₂ adsorption on activated carbons at different CO₂ uptakes

Table S1 Surface area and pore-structure parameters of the activated carbons

Sample	S _{BET} ^[a] (m ² /g)	V _{Micro} ^[b] (cm ³ /g)	V _{total} ^[c] (cm ³ /g)	Pore Size ^[d] (nm)
SK-0.3-700	579	0.23	0.29	2.34
SK-0.5-600	710	0.29	0.44	2.52
SK-0.5-700	1060	0.44	0.52	2.49
SK-0.5-800	1134	0.46	0.68	2.40
SK-0.5-900	1193	0.48	0.71	2.38
SK-1-700	1316	0.55	0.63	2.60
SK-2-700	1395	0.56	0.86	2.47
SK-3-700	2040	0.82	0.89	2.17
SK-4-700	2792	0.92	1.04	2.14

^[a] BET specific surface area. ^[b] Micropore volume calculated by modern NLDFT method. ^[c] Single point total pore volume measured at p/p⁰ = 0.995. ^[d] Pore size = 4V_{total}/S_{BET}.

Table S2 Surface composition of the activated carbons

sample	Concentration (mmol/g)					
	Total N	Pyridine	PhNH ₂ /–C=NH	Pyrrole	Quaternary N	Oxynitride
SK-0.3-700	0.31	0.048	0.072	0.106	0.06	0.024
SK-0.5-600	0.25	0.038	0.058	0.089	0.056	0.009
SK-0.5-700	0.2	0.034	0.056	0.072	0.033	0.005
SK-0.5-800	0.11	0.007	0.03	0.035	0.022	0.016
SK-0.5-900	0.08	0.018	0.016	0.013	0.008	0.025
SK-4-700	0.13	0.029	0.005	0.004	0.082	0.01

Table S3 The total energies for NCSM-CO₂ and CSM-CO₂ complexes ^[a]

Species	$E_{\text{zero}}(\text{a.u.})$	E_{total} (a.u.)	ΔE_i (kJ/mol)	Species	$E_{\text{zero}}(\text{a.u.})$	E_{total} (a.u.)	ΔE_i (kJ/mol)
NCSM	0.326922	-1384.8532479	---	CSM	0.392071	-1230.3673953	---
NCSM -CO ₂ -1	0.338920	-1573.4464803	7.46	CSM-CO ₂ -1	0.403779	-1418.9583021	1.35
NCSM -CO ₂ -2	0.338858	-1573.4458879	5.90	CSM-CO ₂ -2	0.403665	-1418.9583340	1.43
NCSM -CO ₂ -3	0.338844	-1573.4465088	7.53	CSM-CO ₂ -3	0.403710	-1418.9580147	0.60
NCSM -CO ₂ -4	0.338789	-1573.4459003	5.93	CSM-CO ₂ -4	0.403790	-1418.9584483	1.73
NCSM -CO ₂ -5	0.338903	-1573.4468563	8.44	CSM-CO ₂ -5	0.403716	-1418.9582739	1.28
NCSM -CO ₂ -6	0.338757	-1573.4457918	5.65	CSM-CO ₂ -6	0.403642	-1418.9580932	0.80
NCSM -CO ₂ -7	0.339117	-1573.4480562	11.59	CSM-CO ₂ -7	---	---	---
NCSM -CO ₂ -8	0.339101	-1573.4475194	10.18	CSM-CO ₂ -8	0.403608	-1418.9584041	1.62

^[a] $E(\text{CO}_2)$: -188.5903926 a.u.; $\Delta E_i = [E_{\text{total}}(\text{M})+E(\text{CO}_2)]-E_{\text{total}}(\text{M}-\text{CO}_2-i)$, where M represents NCSM or CSM, and i represents 1,2,3,4,5,6,7,8; ΔE_i is equal to hydrogen bond energy.

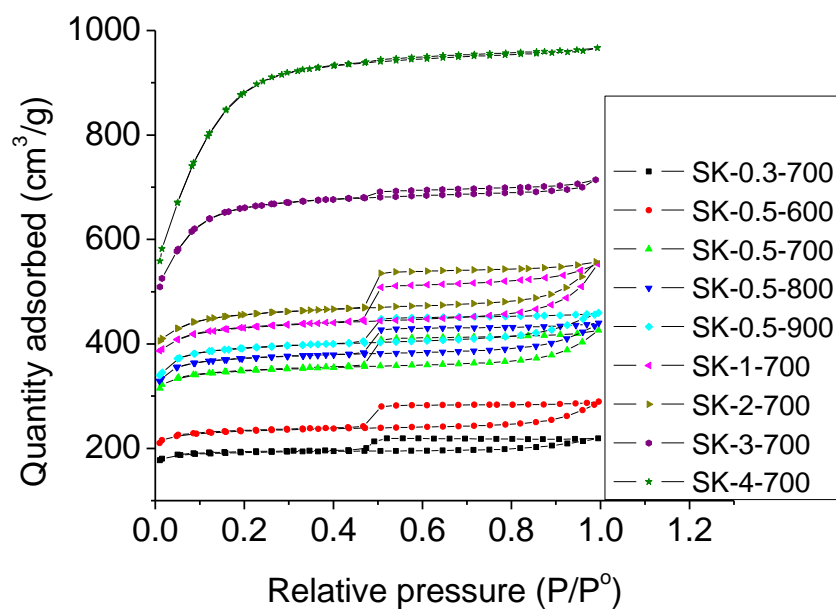


Figure S1 N₂ adsorption isotherms for all the carbons investigated

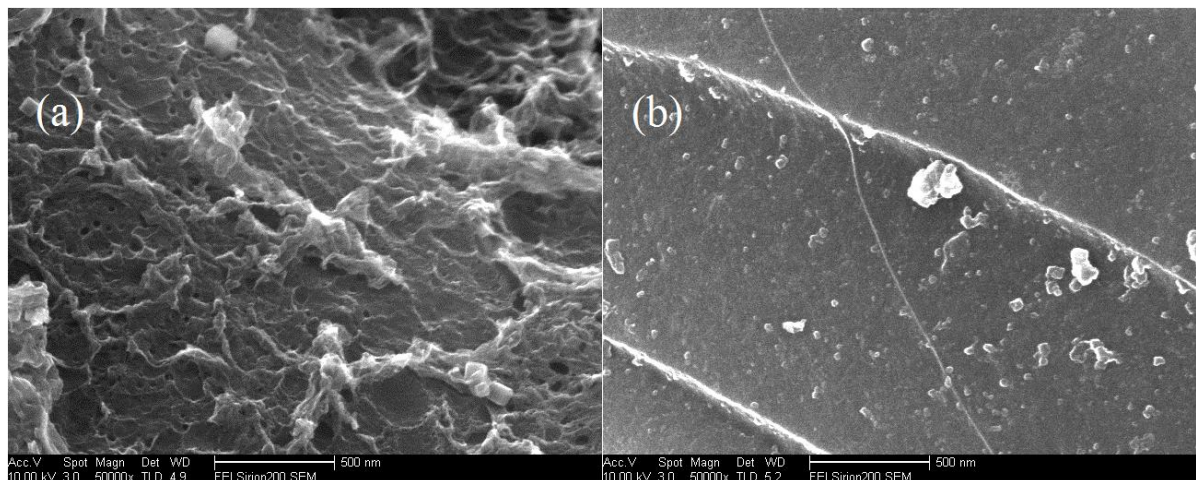


Figure S2 SEM images of (a) SK-0.5-700 and (b) SK-4-700

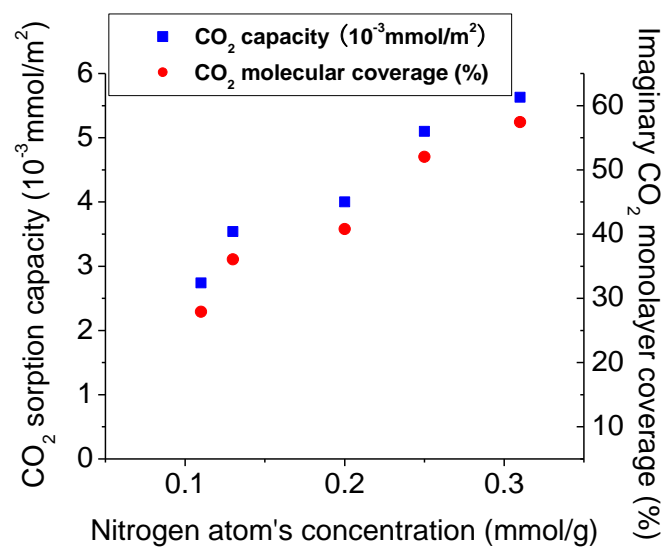


Figure S3 The plot of CO_2 adsorption capacity per unit surface area and imaginary CO_2 monolayer coverage on the surface of carbon versus the nitrogen content of the carbons

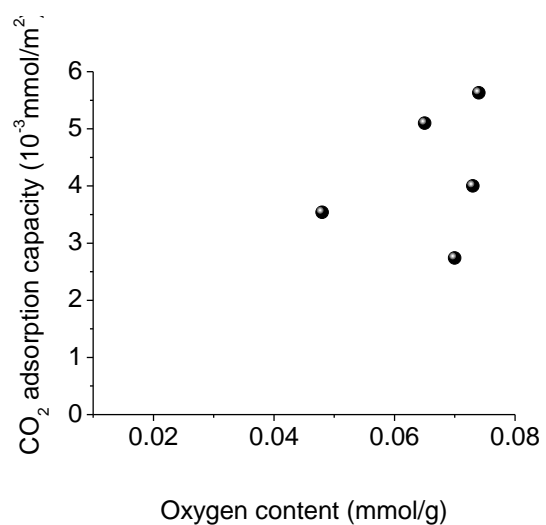
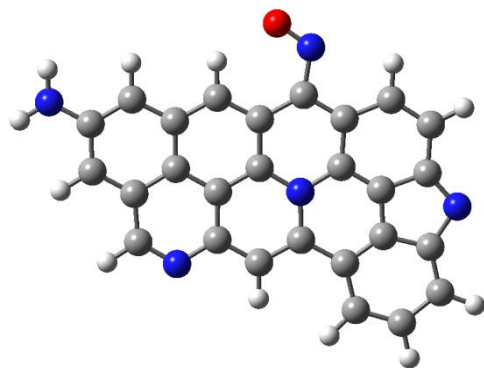
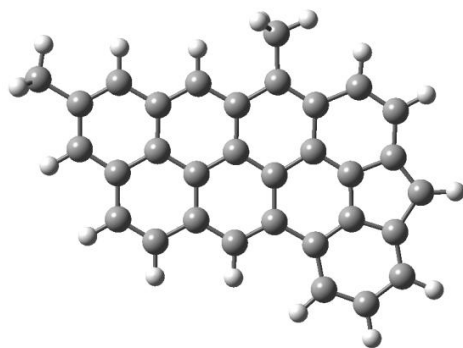


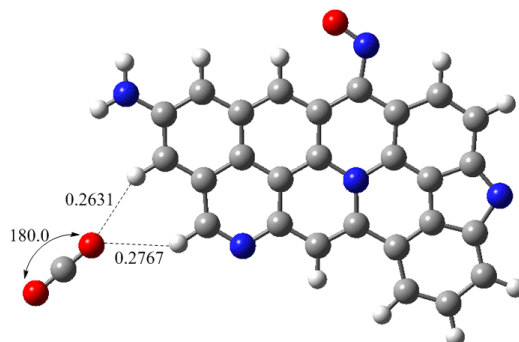
Figure S4 A plot of CO₂ adsorption capacities vs. oxygen contents of the carbons



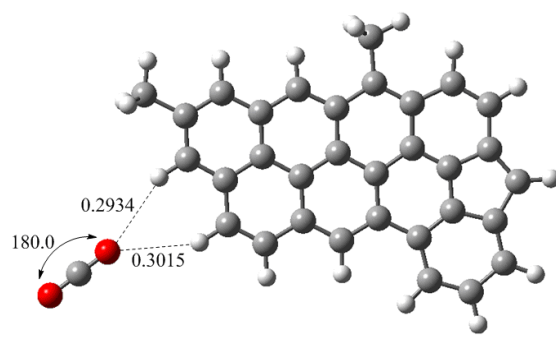
NCSM: E=-1384.8532479 a.u.



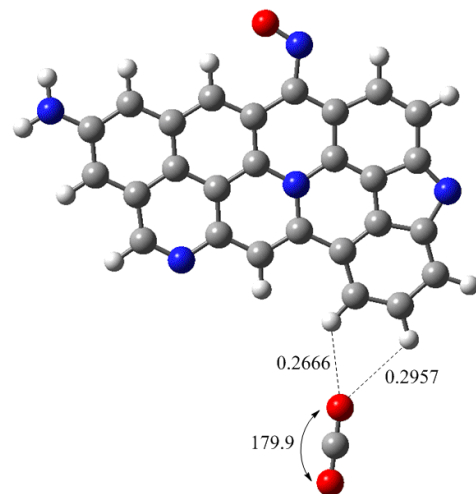
CSM: E=-1230.3673953 a.u.



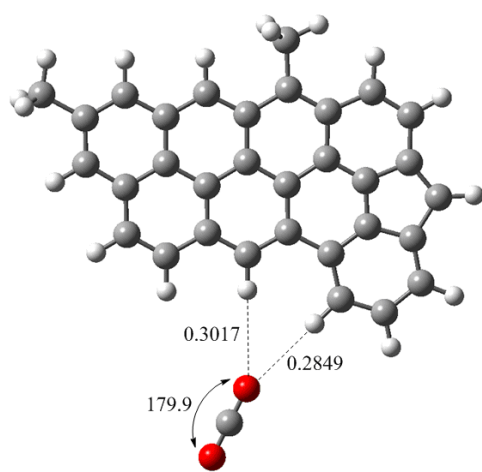
NCSM-CO₂-1: E= -1573.4464803 a.u.



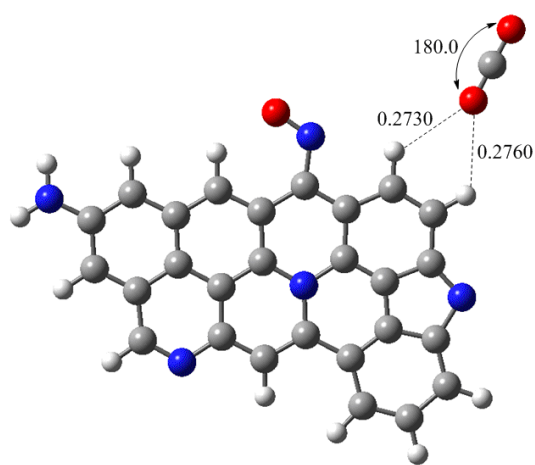
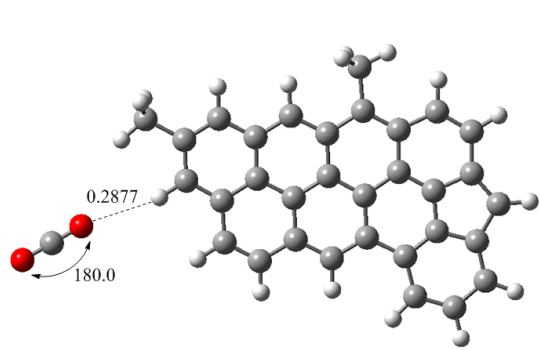
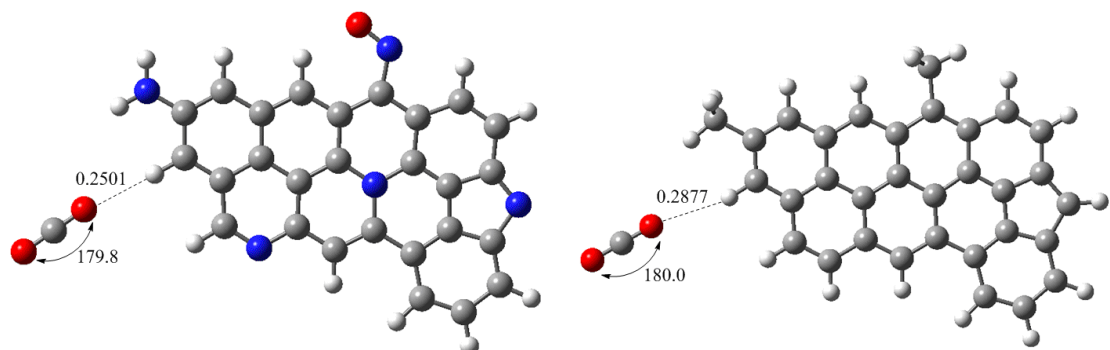
CSM-CO₂-1: E= -1418.9583021 a.u.



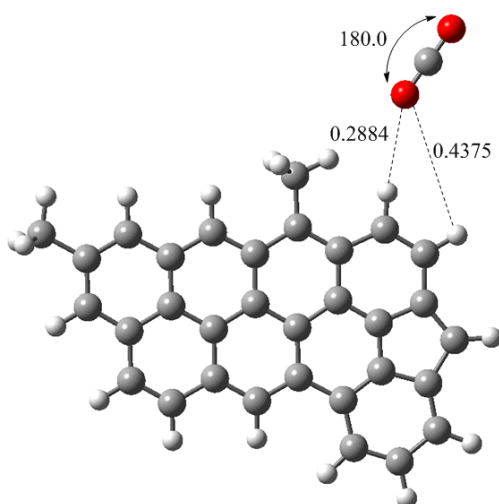
NCSM-CO₂-2: E= -1573.4458879 a.u.



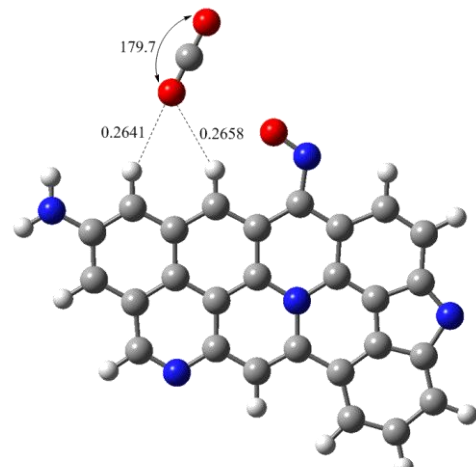
CSM-CO₂-2: E= -1418.9583340 a.u.



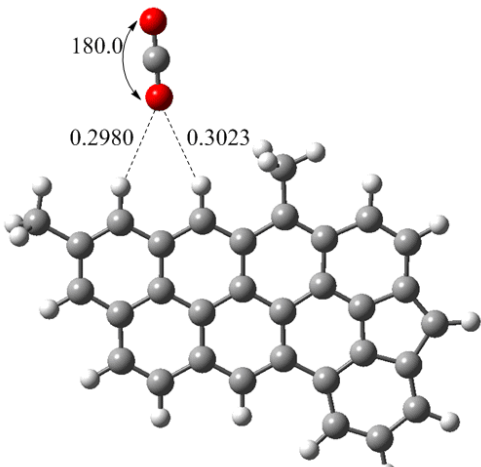
NCSM-CO₂-4: E= -1573.4459003 a.u.



CSM-CO₂-4: E= -1418.9584483 a.u.



NCSM-CO₂-5: E= -1573.4468563 a.u.



CSM-CO₂-5: E= -1418.9582739 a.u.

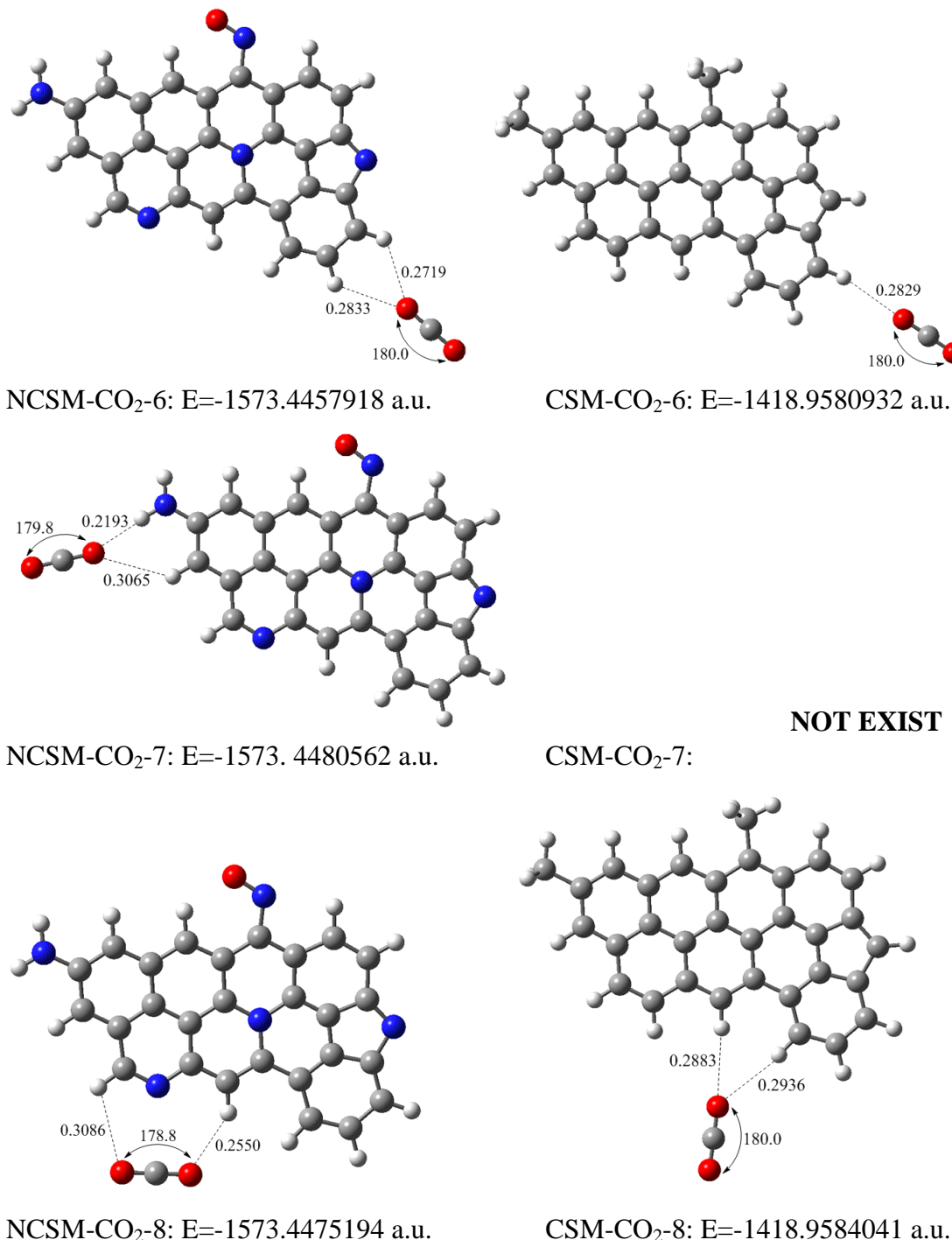


Figure S5 Geometric configurations and total energies for NCSM, CSM, NCSM-CO₂ complexes and CSM-CO₂ complexes simulated by Gaussian03 package ^[1]. (red ball: oxygen atom; blue ball: nitrogen atom; grey ball: carbon atom; small grey ball: hydrogen atom). The units for bond length and bond angle are nm and degree, respectively.

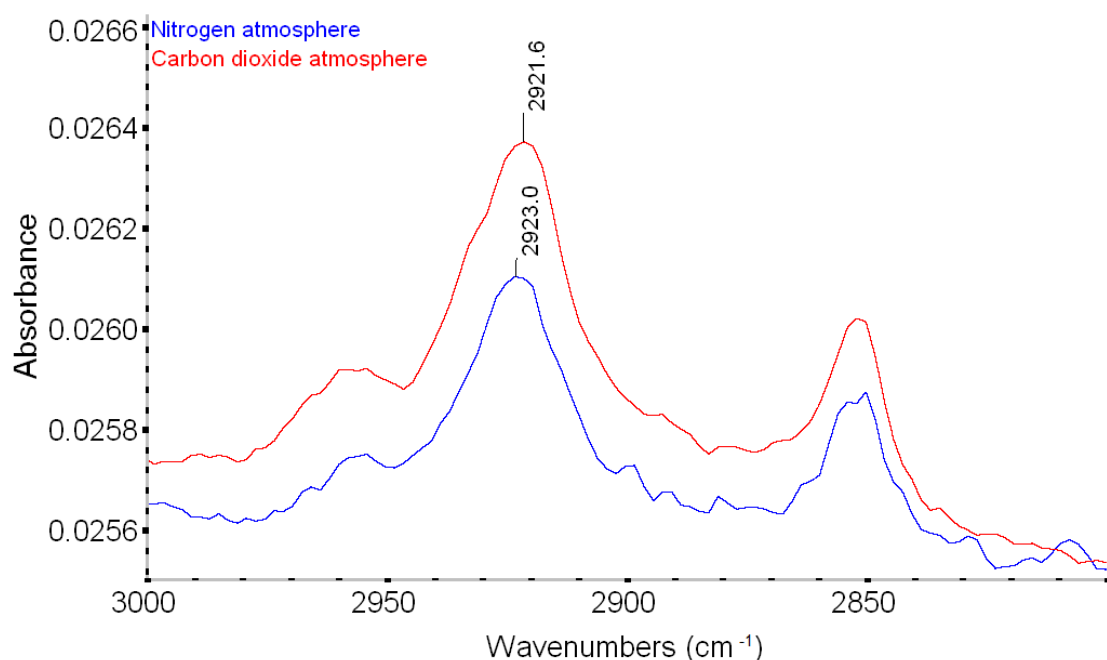


Figure S6 FT-IR spectra of the activated carbon measured under different atmosphere

The infrared spectra of SK-0.3-700 were recorded under N₂ and CO₂ atmosphere, respectively, using a Nicolet 5700 infrared spectrometer with an accuracy of 0.1 cm⁻¹. Under N₂ atmosphere, the peak at 2923.0 cm⁻¹ was attributed to the C-H anti-symmetric stretching vibration. When the atmosphere was switched to CO₂, this peak was broadened and red-shifted to 2921.6 cm⁻¹. It is reported that hydrogen-bonding interactions can weaken the C-H bond energy, which results in the peak widening and red-shift of corresponding peak in FT-IR spectra.^[2, 3] This phenomenon proved that hydrogen-bonding interactions do exist between carbon surface and CO₂ molecules, which is well fitted with the quantum chemical calculations conducted in this work.

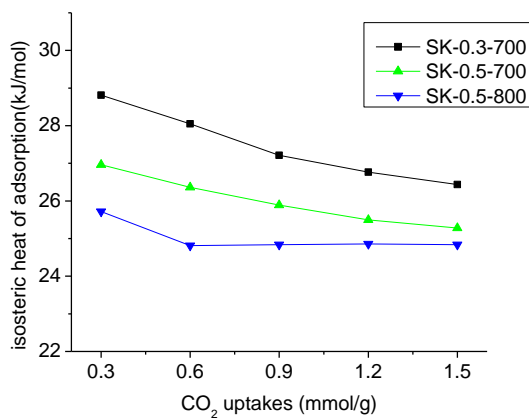


Figure S7 Isosteric heats of CO₂ adsorption on activated carbons at different CO₂ uptakes

The isosteric heats of adsorption were calculated according to Clausius-Clapeyron equation:

$$\ln\left(\frac{p_1}{p_2}\right) = Q_{st} \times \frac{T_2 - T_1}{R \times T_1 \times T_2} \quad (1)$$

where Q_{st} is the isosteric heats of adsorption, T_i represents a temperature at which an isotherm i is measured, p_i represents a pressure at which a specific equilibrium adsorption amount is reached at T_i , R is gas constant (8.314 J/(K mol⁻¹)). As is shown in Figure S7, the isosteric heats of CO₂ adsorption on the carbons are between 24 to 30 kJ/mol. The isosteric heat of adsorption of SK-0.3-700 (with N content of 0.31 mmol/g) is higher than that of SK-0.5-800 (with N content of 0.11 mmol/g) by 1.5~3 kJ/mol, which roughly agrees with the calculated binding energy difference (about 6.5 kJ/mol) between NCSM-CO₂ and CSM-CO₂ complexes. This energy difference indicates that N-doping on carbon surface will increase the isosteric heat of CO₂ adsorption by about 6.5 kJ/mol.

The binding energies for NCSM-CO₂ or CSM-CO₂ complexes are calculated based on interactions between a ideal graphene-like model and CO₂ molecules. In contrast, CO₂ adsorption on micropore surface is apparently different from what is depicted by this ideal interacting model. As is well known, micropores have strong adsorption potential, resulting in high heat of gas adsorption on micropores. That is to say, the binding energies for NCSM-CO₂ or CSM-CO₂ complexes can not reflect the absolute value of adsorption heat on micropores, but somehow reflect the effect of N-doping on heat of gas adsorption.

References

- [1] M.J. Frisch, G.W. Trucks, H.B. Schlegel, G.E. Scuseria, M.A. Robb, J.R. Cheeseman, J.A. Montgomery Jr., T. Vreven, K.N. Kudin, J.C. Burant, J.M. Millam, S.S. Iyengar, J. Tomasi, V. Barone, B. Mennucci, M. Cossi, G. Scalmani, N. Rega, G.A. Petersson, H. Nakatsuji, M. Hada, M. Ehara, K. Toyota, R. Fukuda, J. Hasegawa, M. Ishida, T. Nakajima, Y. Honda, O. Kitao, H. Nakai, M. Klene, X. Li, J.E. Knox, H.P. Hratchian, J.B. Cross, V. Bakken, C. Adamo, J. Jaramillo, R. Gomperts, R.E. Stratmann, O. Yazyev, A.J. Austin, R. Cammi, C. Pomelli, J.W. Ochterski, P.Y. Ayala, K. Morokuma, G.A. Voth, P. Salvador, J.J. Dannenberg, V.G. Zakrzewski, S. Dapprich, A.D. Daniels, M.C. Strain, O. Farkas, D.K. Malick, A.D. Rabuck, K. Raghavachari, J.B. Foresman, J.V. Ortiz, Q. Cui, A.G. Baboul, S. Clifford, J. Cioslowski, B.B. Stefanov, G. Liu, A. Liashenko, P. Piskorz, I. Komaromi, R.L. Martin, D.J. Fox, T. Keith, M.A. Al-Laham, C.Y. Peng, A. Nanayakkara, M. Challacombe, P.M.W. Gill, B. Johnson, W. Chen, M.W. Wong, C. Gonzalez, J.A. Pople, Gaussian03, Revision C.02, Gaussian, Inc., Wallingford, CT, 2003.
- [2] M. H. Jeng, A. M. DeLaat, B. S. Ault, *J. Phys. Chem.* **1989**, *93*, 3997.
- [3] M. Rozenberg, A. Loewenschuss, Y. Marcus, *Phys. Chem. Chem. Phys.* **2000**, *2*, 2699.